Reevaluation of thermonuclear reaction rate of ^{50}Fe(p, γ)^{51}Co *

Li-Ping Zhang(张立萍)[1] Jian-Jun He(何建军)[2;1)]
Wan-Dong Chai(柴万东)[1] Su-Qing Hou(侯素青)[3] Li-Yong Zhang(张立勇)[3]

[1] College of Physics and Electronic Information Engineering, Chifeng University, Chifeng 024000, China
[2]Key Laboratory of Optical Astronomy, National Astronomical Observatories, Chinese Academy of Sciences, Beijing 100012, China
[3] Institute of Modern Physics, Chinese Academy of Sciences, Lanzhou 730000, China

Abstract: The thermonuclear rate of the ^{50}Fe(p, γ)^{51}Co reaction in the Type I X-ray bursts (XRBs) temperature range has been reevaluated based on a recent precise mass measurement at CSRe Lanzhou, where the proton separation energy $S_{\rm p}$=142±77 keV has been determined firstly for the ^{51}Co nucleus. Comparing to the previous theoretical predictions, the experimental $S_{\rm p}$ value has much smaller uncertainty. Based on the nuclear shell model and mirror nuclear structure information, we have calculated two sets of thermonuclear rates for the ^{50}Fe(p, γ)^{51}Co reaction by utilizing the experimental $S_{\rm p}$ value. It shows that the statistical-model calculations are not ideally applicable for this reaction primarily because of the low density of low-lying excited states in ^{51}Co. In this work, we recommend that a set of new reaction rates based on the mirror structure of ^{51}Cr should be incorporated in future astrophysical network calculations.

Keywords: X-ray burst (XRB), nucleosynthesis, mass measurement, proton separation energy, reaction rate

PACS: 21.10.-k,21.60.Cs,26.30.+k **DOI:** 10.1088/1674-1137/40/12/125101

1 Introduction

Type I X-ray bursts (XRBs) arise from thermonuclear runaways on the accreted envelopes of neutron stars in close binary systems [1, 2]. During the thermonuclear runaway, an accreted envelope enriched in H and He may be transformed to matter strongly enriched in heavier species (up to $A\sim$100 [3, 4]) via the rapid proton capture process (rp-process) [5–7]. Please see, e.g., Refs. [8–10] for reviews on XRBs.

The rp-process is largely characterized by localized (p,γ)-(γ,p) equilibrium within particular isotonic chains near the proton drip-line. In such an equilibrium situation the abundance distribution within an isotonic chain depends exponentially on nuclear mass differences as the abundance ratio between two neighboring isotones is proportional to exp[$S_{\rm p}/kT$] ($S_{\rm p}$: proton separation energy, T: temperature of the stellar environment). In particular, those isotonic chains with sufficiently small $S_{\rm p}$ values (relative to XRB temperatures - at 1 GK, $kT\approx$100 keV) need to be known with a precision of at least 50−100 keV [6, 11]. In order to compare model predictions with observations of the light curves [12], reliable nuclear-physics inputs, e.g., precise $S_{\rm p}$ values and nuclear structure information, are needed for those nuclei along the rp-process path.

Recently, precise mass measurements of nuclei along the rp-process path have become available. These measurements were made at the HIRFL-CSR (Cooler-Storage Ring at the Heavy Ion Research Facility in Lanzhou) [13] in IMS (Isochronous Mass Spectrometry) mode. The proton separation energy of ^{51}Co has been experimentally determined to be $S_{\rm p}^{\rm IMP}$=142±77 keV for the first time [14]. Although the estimated values in the previous Atomic Mass Evaluations (i.e., $S_{\rm p}$=240±210 keV in AME85 [15], 290±160 keV in AME93 [16], 90±160 keV in both AME95 [17] and AME03 [18]) agree with this experimental value within 1 σ uncertainty, the experimental value is significantly more precise.

Previously, the impact of Q-value (i.e., $S_{\rm p}$ value) for the ^{50}Fe(p, γ)^{51}Co reaction was studied [11] based on the old $S_{\rm p}$(^{51}Co) value of AME03. In the XRB 'short' model, it shows that the uncertainty of Q-value has very large impact on the final yields of ^{51}Cr and ^{52}Fe, whose yields can be significantly affected by factors of 4.9 and 2.0, respectively, by changing Q to $Q+\Delta Q$. Therefore, a precise $S_{\rm p}$ (^{51}Co) value is very important for constraining the final XRB yields. In this work, we have derived

Received 25 July 2016, Revised 19 September 2016

∗ Supported by Natural Science Foundation of Inner Mongolia Autonomous Region of China (2013MS0916) and National Natural Science Foundation of China (11490562, 11405228)

1) E-mail: hejianjun@nao.cas.cn

the thermonuclear rates of ^{50}Fe(p, γ)^{51}Co based on the new experimental $S_{\rm p}$ (^{51}Co) value, with which the resonant and direct capture (DC) rates are recalculated. This precise $S_{\rm p}$ value allows the uncertainty in the rate of the ^{50}Fe(p, γ)^{51}Co reaction to be dramatically reduced (e.g., see Ref. [19]), and hence the XRB yields can be well constrained too.

2 Previous reaction rates

2.1 Available rates

The thermonuclear rate of the ^{50}Fe(p, γ)^{51}Co reaction was firstly estimated by Van Wormer et al. [20] based entirely on the properties of 6 resonances in the mirror nucleus ^{51}Cr, because of no experimental level structure of ^{51}Co available. A value of $S_{\rm p}$=240 keV estimated from AME85 was utilized in that paper. This rate was estimated later [21] with a statistical-model code using the Hauser-Feshbach formalism (NON-SMOKER [22]) based on the different $S_{\rm p}$ values of ^{51}Co predicted by the finite-range droplet macroscopic model (FRDM) [23] ($S_{\rm p}$=1.369 MeV) and ETSFIQ mass model [24] ($S_{\rm p}$=1.659 MeV). Later on, this rate was calculated by Fisker et al. [25] under a framework of shell model with a value of $S_{\rm p}$=90 keV from AME95. In addition, some theoretical rates calculated using statistical models are available in JINA REACLIB[1)] [26], which were estimated by the statistical model with different $S_{\rm p}$ values. The predicted rates differ from one another by up to several orders of magnitude over the typical XRB temperatures. Moreover, the mirror ^{51}Cr nucleus exhibits a low level-density structure near the proton threshold of ^{51}Co, and therefore the reliability of such statistical model calculations may be questionable.

Below, we refer to previously available rates using the nomenclature adopted in the JINA REACLIB database. Explicitly, the laur rate refers to exactly the rate estimated by Ref. [20]; the rath rate adopts exactly the one calculated by Ref. [21]. The rath, thra rates are the statistical-model calculations with FRDM and ETSFIQ masses, respectively. The recent ths8 rate is the theoretical one from T. Rauscher [26]. In addition, the rate calculated by Fisker et al. [25] was revised with a value of $S_{\rm p}$=355 keV, and referred to as nfis in JINA REACLIB [26].

2.2 Existing problems

By a careful survey, we find that there were several mistakes made in the previous paper of Fisker et al. [25]. In general, the direct-capture (DC) rate, which was expressed by their Eq. (15), should be multiplied by a factor of 2. Concerning the ^{50}Fe(p, γ)^{51}Co reaction, we have recalculated all the rates (DC, resonant and total ones) by utilizing the parameters listed in their Table I (p. 261), and the comparison is made in Table 1. It can be seen that all rates listed in Table I (p. 286) of Ref. [25] are significantly different from the present ones, and it implies that some mistakes were made in the previous work. Unfortunately, we cannot find the exact source of these errors.

Table 1. Ratio of reaction rates between present and previous calculations [25].

	ratio (present/previous)		
T9	DC rate[a]	resonant rate[b]	total rate
0.1	9.8E-02	3.4E+08	3.4E+08
0.2	6.4E-02	4.6E+04	2.5E+04
0.3	5.3E-02	1.1E+00	1.1E+00
0.4	4.8E-02	1.3E+00	1.3E+00
0.5	4.4E-02	1.4E+00	1.4E+00
0.6	4.2E-02	1.3E+00	1.3E+00
0.7	4.0E-02	1.3E+00	1.3E+00
0.8	3.9E-02	1.2E+00	1.2E+00
0.9	3.8E-02	1.2E+00	1.2E+00
1.0	3.7E-02	1.1E+00	1.1E+00
2.0	3.2E-02	8.9E-01	7.9E-01
3.0	3.0E-02	9.4E-01	6.0E-01
4.0	2.9E-02	9.8E-01	4.8E-01
5.0	2.8E-02	9.9E-01	3.6E-01
6.0	2.7E-02	9.9E-01	2.5E-01
7.0	2.7E-02	9.9E-01	1.8E-01
8.0	2.7E-02	9.9E-01	1.3E-01
9.0	2.6E-02	9.9E-01	9.5E-02
10.0	2.6E-02	9.9E-01	7.3E-02

[a]: Calculated by the analytical Eq. (15) of Ref. [25] with an enhanced factor of 2 as explained in the text.

[b]: Calculated by the analytical Eq. (7) of Ref. [25] with exactly the same parameters as listed in Table I.

In addition, Van Wormer et al. [20] estimated the ^{50}Fe(p, γ)^{51}Co reaction rate relying on 6 resonances in the mirror ^{51}Cr, and neglected the DC contributions. They used a value of $S_{\rm p}$=240 keV adopted from AME85. In fact, only two resonances, i.e., at E_r=0.51, 0.92 MeV, dominate the total resonant rate; the former contributes the rate below 0.4 GK, while the latter overwhelmingly contributes in the region of 0.4−2 GK. We have reproduced very well (less than 5% deviation) the strength $\omega\gamma$ values for the five resonances (i.e., $E_{\rm r}$=0.51, 0.53, 1.12, 1.32 and 1.65 MeV) listed in their Table 15 in Ref. [20], with an approximation of $\omega\gamma \approx \omega\Gamma_\gamma$ (since $\Gamma_{\rm p} \gg \Gamma_\gamma$). As for the 'key' resonance at $E_{\rm r}$=0.92 MeV (J^π=9/2$^-$), a value of $\omega\gamma$=3.8×10^{-2} eV was listed in Ref. [20]. With the same approximation of $\omega\gamma \approx \omega\Gamma_\gamma$, we get a strength value about 14% larger than the previous one (we guess

1) http://groups.nscl.msu.edu/jina/reaclib/db

that Van Wormer et al. made the same approximation). According to Eq. (6) of Van Wormer et al., a proton width value of $\Gamma_{\rm p}$=2.08×10^{-6} is obtained for this high-spin 9/2$^-$ (with ℓ=5 transfer) resonance, with a nuclear channel radius of $R=1.26\times(1+50^{\frac{1}{3}})$ fm and an assumed spectroscopic factor of C^2S=0.1. Thus, the above approximation is invalid for this resonance, and its strength is calculated to be 1.04×10^{-5} eV. Now, this 'key' 0.92 MeV resonance makes only negligible contribution to the total rate; the 0.51 MeV resonance dominates the total rate below ∼1 GK, while the 1.12 MeV resonance dominates the rate in the temperature region of 1−2 GK.

3 New reaction rates

In this work, we will use the new experimental value of $S_{\rm p}^{\rm IMP}(^{51}{\rm Co})$=142±77 keV to recalculate the thermonuclear reaction rate of ^{50}Fe(p, γ)^{51}Co. As for a typical (p, γ) reaction, the total thermonuclear reaction rate consists of the resonant and DC rates of proton capture on ground state and all thermally excited states in the target nucleus weighted with their individual population factors [27]. The reaction rates for the ^{50}Fe(p, γ)^{51}Co reaction are calculated as described in the following subsections.

It is well-known that the population of an excited state $E_{\rm x}$ relative to the ground state of the nucleus can be described by the Boltzmann probability function [27]:

$$P(E_{\rm x})=\frac{2J_{\rm r}+1}{2J_0+1}\times\exp\left(-\frac{E_{\rm x}}{kT}\right), \quad (1)$$

where J_0 and $J_{\rm r}$ are the spins of the ground state and excited resonant state, respectively. According to Eq. (1) the probabilities of populating the first-excited state ($E_{\rm x}$=764.9 keV) relative to the ground state in ^{50}Fe are about 1.4×10^{-38} and 0.06 at 0.1 and 2 GK, respectively. Therefore, contributions from these thermally populated excited states can be entirely neglected in the temperature region of XRB interested.

3.1 Resonant rates

In this work, the resonant rate is calculated by Eq. (7) in Ref. [25], i.e., the well-known narrow resonance formalism [20, 27],

$$N_A\langle\sigma v\rangle_{\rm res}=1.54\times10^{11}(AT_9)^{-3/2}\omega\gamma \cdot\exp\left(-\frac{11.605E_r}{T_9}\right)\ ({\rm cm^3\cdot s^{-1}\cdot mol^{-1}}). \quad (2)$$

Here, the resonant energy $E_{\rm r}$ and strength $\omega\gamma$ are in units of MeV. For the proton capture reaction, the reduced mass A is defined by $A_{\rm T}/(1+A_{\rm T})$ (here, target mass $A_{\rm T}$=50 for ^{50}Fe). The resonant strength $\omega\gamma$ is defined by (i.e. Eq. (8) in Ref. [25])

$$\omega\gamma=\frac{2J+1}{2(2J_{\rm T}+1)}\frac{\Gamma_{\rm p}\times\Gamma_\gamma}{\Gamma_{\rm tot}}. \quad (3)$$

Here, $J_{\rm T}$ and J are the spins of the target and resonant state, respectively. $\Gamma_{\rm p}$ is the partial width for the entrance channel, and Γ_γ is that for the exit channel.

Peak temperatures in recent hydrodynamic XRB models have approached 1.5–2 GK [7, 28]. Here, we will consider the reaction rate which holds for a temperature region up to 2.5 GK. For the ^{50}Fe(p, γ)^{51}Co reaction, a temperature of 2.5 GK corresponds to a Gamow peak E_r ≈1.96 MeV with a width of Δ ≈1.50 MeV [27]. Thus, its resonant rate is determined by the resonances with maximum energy up to ∼2.71 MeV. It can be seen that contributions from the resonances presented in the following Tables 2 & 3 are sufficient to account for the resonant rate at XRB temperatures.

3.1.1 Rate based on shell model

In the previous shell-model calculation [25], all the resonant parameters are listed in Table I (see p. 261). Here, we need to recalculate the resonant rate based on the new experimental value of $S_{\rm p}^{\rm IMP}(^{51}{\rm Co})$=142±77 keV. Actually only two quantities need to be changed, i.e., resonance energy $E_{\rm r}$ and proton width $\Gamma_{\rm p}$ (Γ_γ independent on $S_{\rm p}$ value). Resonance energy can be calculated easily by $E_{\rm r}^{\rm Revised}=E_{\rm x}^{\rm Fisker}-S_{\rm p}^{\rm IMP}$. The proton width can be calculated by $\Gamma_{\rm p}^{\rm Revised}=\frac{P_\ell(E_{\rm r}^{\rm Revised})}{P_\ell(E_{\rm r}^{\rm Fisker})}\times\Gamma_{\rm p}^{\rm Fisker}$. Thereinto, the Coulomb penetrability factor P_ℓ can be calculated by the subroutine `RCWFN` [29], with same optical-model parameter (i.e., radius $R=1.26\times(1+50^{1/3})$ fm) as in Refs. [20, 25].

Table 2. Revised resonant parameters based on the previous work [25]. Here, the excitation energy ($E_{\rm x}^{\rm th}$) and resonance energy ($E_{\rm r}$) are in units of keV.

$E_{\rm x}^{\rm th}$	J^π	$E_{\rm r}$	$\Gamma_{\rm p}$/eV	Γ_γ/eV	$\omega\gamma$/eV
839.1	5/2$^-$	697.1	1.14E-05	2.05E-05	2.19E-05
866.7	7/2$^-$	724.7	4.93E-06	5.08E-05	1.80E-05
1720.1	5/2$^-$	1578.1	9.64E-05	6.33E-03	2.85E-04
1857.7	3/2$^-$	1715.7	2.51E+02	1.47E-04	2.93E-04
2076.8	7/2$^-$	1934.8	5.79E-02	2.45E-03	9.42E-03
2583.8	3/2$^-$	2441.8	3.94E+03	1.48E-06	2.96E-06
2597.1	5/2$^-$	2455.1	3.46E+01	3.37E-02	1.01E-01
2636.8	7/2$^-$	2494.8	6.63E-01	5.06E-03	2.01E-02
2937.0	3/2$^-$	2795.0	1.02E+04	1.72E-05	3.44E-05
3041.7	5/2$^-$	2899.7	4.84E+01	1.07E-02	3.22E-02

The resonant parameters are listed in Table 2, and the revised resonant rates (referred to as Res$^{\rm shell}$) in Ta-

ble 4. Our calculation shows that the first two resonances at E_x=839.1, 866.7 keV dominate the total resonant rate up to ∼2 GK, beyond which other two resonances at 2076.8, 2597.1 keV begin to make significant contributions.

3.1.2 Rate based on mirror structure

Alternatively, we have estimated the ^{50}Fe(p, γ)^{51}Co resonant rate by using exactly the level energies, half-lives and single-particle spectroscopic factors from the mirror nucleus ^{51}Cr [30]. A similar approach was utilized in Ref. [19]. Here, the gamma widths (Γ_γ) of the unbound states in ^{51}Co were estimated by the half-lives ($T_{1/2}$) of the corresponding bound states in the mirror ^{51}Cr via Γ_γ=ln(2)×$\hbar/T_{1/2}$; the proton widths were calculated by Eq. (6) in Ref. [20], i.e.,

$$\Gamma_{\rm p} = \frac{3\hbar^2}{AR^2} P_\ell(E) C^2S_{\rm p}. \quad (4)$$

with R=1.26×(1+50$^{\frac{1}{3}}$) fm as the nuclear channel radius, and $C^2S_{\rm p}$ the proton spectroscopic factor of the resonance. Here, we assumed the proton spectroscopic factor in ^{51}Co equal to the neutron spectroscopic factor in the ^{51}Cr mirror, i.e., $C^2S_{\rm p} = C^2S_{\rm n}$. The experimental neutron spectroscopic factors are adopted from the previous (d, p) transfer reactions [31–33]. Here, the spectroscopic factor is a model-dependent quantity (see e.g., Ref. [34]), and its variation may change the proton width $\Gamma_{\rm p}$ accordingly.

Here, we assumed a value of 0.001 for those high-spin states (J^π=9/2$^-$ and 11/2$^-$) listed in Table 3, which have no available experimental C^2S values. Actually, for the states at E_x=1164.6, 2379.5, 2704.4, and 2767.3 keV, their contributions to the total resonant rate are negligible with any values of C^2S<1; for the state at E_x=1480.1 keV, its contributions is negligible with any values under a condition of C^2S<0.1, and we think this condition is appropriate for this J^π=11/2$^-$ state. For the E_x=2828.5 keV state (J^π=3/2$^-$), similarly, its contribution can also be neglected with any values of C^2S<1. Therefore, the states discussed above play only a negligible role in the total resonant rate in spite of assuming any C^2S values. The exception is the E_x=2001.9 keV state (J^π=5/2$^-$) which plays an important role in contributing the total rate. Its resonance strengths are about 80.5, 80.3, 78.3, and 63.1 meV for C^2S values of 1.0, 0.1, 0.01, 0.001, respectively; such variation in strengths cannot be regarded as substantial.

The resonant parameters derived above are listed in Table 3, and the corresponding resonant rates (referred to as Res$^{\rm mirror}$) in Table 4. The contributions of each resonance to the total resonant rate have been calculated, and the role for those important resonances is shown in Fig. 1. It shows that three key resonances (i.e., at E_x=749.1, 1352.7 and 2001.9 keV) dominate the total resonant rate in the temperature region of 0.1–2.5 GK.

Table 3. Resonant parameters based on the nuclear structure in mirror ^{51}Cr. The excitation energy E_x, spin-parity J^π, and half-life $T_{1/2}$ are taken from Ref. [30]. The spectroscopic factor values of $C^2S_{\rm p}$ are the averaged ones from the previous (d, p) experiments [31–33], except the assumed value of 0.001.

E_x/keV	E_r^a/keV	J^π	$T_{1/2}$/ps	$C^2S_{\rm p}$	Γ_γ^b/eV	$\Gamma_{\rm p}$/eV	$\omega\gamma$/eV
749.1	607.1	3/2$^-$	3300	0.36	1.38E-07	2.48E-03	2.76E-07
776.9	634.9	1/2$^-$	6900	0.29	6.61E-08	4.12E-03	6.61E-08
1164.6	1022.6	9/2$^-$	0.076	0.001	6.00E-03	9.64E-08	4.82E-07
1352.7	1210.7	5/2$^-$	3.8	0.17	1.20E-04	1.57E-01	3.60E-04
1480.1	1338.1	11/2$^-$	0.55	0.001	8.29E-04	3.56E-06	2.13E-05
1557.3	1415.3	7/2$^-$	4.2	0.09	1.09E-04	4.78E-01	4.34E-04
1899.2	1757.2	3/2$^-$	0.29	0.16	1.57E-03	5.47E+02	3.15E-03
2001.9	1859.9	5/2$^-$	0.017	0.001	2.68E-02	9.74E-02	6.31E-02
2312.6	2170.6	7/2$^-$	0.015	0.01	3.04E-02	4.59E+00	1.21E-01
2379.5	2237.5	9/2$^-$	0.31	0.001	1.47E-03	1.42E-03	3.62E-03
2704.4	2562.4	(11/2$^-$)	0.085	0.001	5.37E-03	5.83E-03	1.68E-02
2762.6	2620.6	1/2$^+$	0.071	0.02	6.42E-03	2.53E+03	6.42E-03
2767.3	2625.3	9/2$^-$	0.041	0.001	1.11E-02	7.45E-03	2.23E-02
2828.5	2686.5	3/2$^-$	0.059	0.001	7.73E-03	9.29E+01	1.55E-02
2890.2	2748.2	3/2$^-$	0.35	0.10	1.30E-03	1.03E+04	2.61E-03
2911.0	2769.0	(3/2$^-$,5/2,7/2$^-$)	0.03	0.06	1.52E-02	1.86E+02^f	4.56E-02
2948.2	2806.2	5/2$^-$,7/2$^-$	0.119	0.04	3.83E-03	1.63E+02	1.15E-02

^{a}: Calculated by $E_r = E_x - S_{\rm p}^{\rm IMP}$ with $S_{\rm p}^{\rm IMP}$=142 keV [14].

^{b}: Calculated by Γ_γ=ln(2)×$\hbar/T_{1/2}$.

^{f}: Assuming an ℓ=3 transfer.

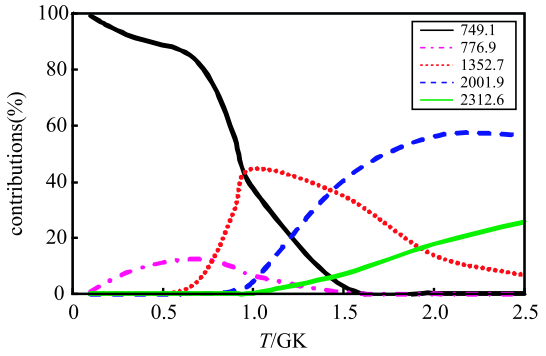

Fig. 1. (color online) Percentage contribution of resonances to the total resonant rate. Here, 5 resonances (listed in Table 3) which have significant contribution (>10%) are shown, with E_x energies indicated in the legend.

3.2 DC rate

The nonresonant direct-capture (DC) rate can be estimated by the following expression [27],

$$N_A\langle\sigma v\rangle_{\rm DC} = 7.83\times10^9\left(\frac{Z_{\rm T}}{A}\right)^{1/3} T_9^{-2/3} S_{\rm DC}^{\rm eff}(E_0) \times\exp\left[-4.249\left(\frac{Z_{\rm T}^2 A}{T_9}\right)^{1/3}\right] \quad ({\rm cm^3\cdot s^{-1}\cdot mol^{-1}}), \tag{5}$$

with $Z_{\rm T}$ being the atomic number of ^{50}Fe. The effective astrophysical S-factor at the Gamow energy E_0, i.e., $S_{\rm DC}^{\rm eff}(E_0)$, is usually approximated by [25, 27],

$$S_{\rm DC}^{\rm eff}(E_0) = S(0)\left(1+\frac{5}{12\tau}\right), \tag{6}$$

where $S(0)$ is the S-factor at zero energy. It should be noted that the direct-capture rate expressed by Eq. (15) in Ref. [25] should be multiplied by a factor of 2.

In this work, we have calculated the ^{50}Fe(p, γ)^{51}Co DC S-factors with a RADCAP code [35]. The Woods-Saxon nuclear potential (central + spin orbit) and a Coulomb potential of uniform-charge distribution were utilized in the calculation. The nuclear central potential V_0 were determined by matching the bound-state energies. The optical-potential parameters [25] are $R_0 = R_{\rm s.o.} = R_{\rm C} = 1.25\times(1+A^{\frac{1}{3}})$ fm, $a_0 = a_{\rm s.o.} = 0.6$ fm, with a depth of spin-orbit potential of $V_{\rm s.o.} = -10$ MeV. Here, R_0, $R_{\rm s.o.}$ and $R_{\rm C}$ are radii of central potential, spin-orbit potential and Coulomb potential, respectively; a_0 and $a_{\rm s.o.}$ are the corresponding diffuseness in central and spin-orbit potentials, respectively. We have reproduced the previous value of $S(0)$=0.1313 [MeV b] with a spectroscopic factor of C^2S=0.22, by using the same optical-model parameters and an $S_{\rm p}$ value of 90 keV as in Ref. [25]. This spectroscopic factor can be found in the Ref. [31].

Here, we adopted an averaged spectroscopic factor of C^2S=0.29 for the ground-state capture [31–33], together with the new experimental value of $S_{\rm p}^{\rm IMP}$=142(77) keV and the same optical-model parameters of Ref. [25]. A value of $S(0)$=0.1896 (MeV·b) is obtained for the DC capture. The presently calculated $S_{\rm DC}$ factors can be well parameterized in a Taylor-series form Ref. [27] of $S_{\rm DC}(E) = S(0)+\dot{S}(0)E+\frac{1}{2}\ddot{S}(0)E^2$, where S factor are in units of [MeV b] and E in MeV. The fitted parameters are $S(0)$=0.1896 [MeV b], $\dot{S}(0)$=5.897×10^{-2} (MeV^{-1}) and $\ddot{S}(0)$=4.787×10^{-2} (MeV^{-2}), respectively. According to the textbook [27], the effective astrophysical S-factor at the Gamow energy E_0 in the above Eq. (5) can be expressed as the well-known formulism [27],

$$S_{\rm DC}^{\rm eff}(E_0) = S(0)\left[1+\frac{5}{12\tau}+\frac{\dot{S}(0)}{S(0)}\left(E_0+\frac{35}{36}kT\right) +\frac{1}{2}\frac{\ddot{S}(0)}{S(0)}\left(E_0^2+\frac{89}{36}E_0kT\right)\right]. \tag{7}$$

The DC reaction rates calculated with the approximated Eq. (6) are compared to those with the more precise Eq. (7), and we find that the latter are larger than the former by factors of about 1.1, 2.5, and 7.0 at 0.1, 3, and 10 GK, respectively; the latter are consistent very well with the numerical integration method by using an EXP2RATE code [36]. Thus, we have calculated the DC rates with Eqs. (5) & (7) as listed in Table 4.

Table 4. Presently calculated resonant and DC rates for the ^{50}Fe(p, γ)^{51}Co reaction, in units of cm^3·s^{-1}·mol^{-1}.

T_9	DC	Res$^{\rm shell}$	Res$^{\rm mirror}$
0.10	4.89E-25	8.26E-34	3.49E-31
0.15	9.22E-21	2.46E-22	3.06E-21
0.20	4.58E-18	1.21E-16	2.55E-16
0.30	1.10E-14	5.22E-11	1.80E-11
0.40	1.49E-12	3.06E-08	4.25E-09
0.50	4.89E-11	1.31E-06	1.05E-07
0.60	7.05E-10	1.53E-05	8.54E-07
0.70	5.94E-09	8.54E-05	3.82E-06
0.80	3.46E-08	3.02E-04	1.26E-05
0.90	1.54E-07	7.92E-04	3.64E-05
1.00	5.56E-07	1.68E-03	1.00E-04
1.50	5.31E-05	1.46E-02	7.52E-03
2.00	9.66E-04	4.99E-02	1.28E-01
2.50	7.73E-03	1.72E-01	7.85E-01

In addition, the parameter dependence on $S_{\rm DC}(E)$ has been studied for this reaction. The sensitivities are about: 80% on R_0 (4.64−5.86 fm, i.e., $1.25\times(1+50)^{\frac{1}{3}}$=4.64 fm [37], $1.25\times(1+50^{\frac{1}{3}})$=5.86 fm [25]), 12% on $V_{\rm s.o.}$ (0−−10 MeV [37]), 10% on $S_{\rm p}$ error (±77 keV), and 8% on a (0.55 0.65 fm), respectively.

The uncertainties of the derived S factors and DC rates are about a factor of 3.

Comparing the resonant rates and DC rate listed in Table 4, it shows that the DC contribution dominate the total rate below 0.15 GK, beyond which the resonant capture makes the overwhelming contribution. Our result is significantly different from the previous conclusion [25].

3.3 Total reaction rates

The total reaction rate of ^{50}Fe(p,γ)^{51}Cr has been calculated by simply summing up the resonant and DC rates as discussed above. Two sets of total rates, referred to as shell and mirror, are tabulated in Table 5. The present mirror rate can be well parameterized by the standard format of [21]:

$$N_A\langle\sigma v\rangle = \exp\Big(687.603-\frac{9.111}{T_9}+\frac{575.394}{T_9^{1/3}} -1378.820T_9^{1/3}+128.398T_9-13.263T_9^{5/3} +549.246\ln T_9\Big)+\exp\Big(578.307-\frac{16.326}{T_9} +\frac{541.104}{T_9^{1/3}}-1223.680T_9^{1/3}+123.472T_9 -12.881T_9^{5/3}+475.982\ln T_9\Big) \quad (8)$$

with fitting error of less than 0.6% in 0.1–2.5 GK; the present shell rate can be expressed as,

$$N_A\langle\sigma v\rangle = \exp\Big(2129.450+\frac{20.158}{T_9}-\frac{1028.750}{T_9^{1/3}} -2426.040T_9^{1/3}+2276.410T_9-1051.510T_9^{5/3} -325.917\ln T_9\Big)+\exp\Big(-254.347-\frac{5.474}{T_9} -\frac{179.555}{T_9^{1/3}}+485.685T_9^{1/3}-61.715T_9 +9.015T_9^{5/3}-173.845\ln T_9\Big) \quad (9)$$

with fitting error of less than 0.5% in 0.1–2.5 GK. We emphasize that the above fits are only valid within the stated errors over the temperature range of 0.1–2.5 GK. Above 2.5 GK, one may, for example, match our rates to those statistical model calculations.

Table 5. Thermonuclear rates of ^{50}Fe(p,γ)^{51}Co. The adopted $S_{\rm p}$ values are listed in the parentheses.

	present rates		JINA REACLIB rates				
	mirror	shell	nfis	rath	thra	ths8	laur
T_9	(0.142 MeV)	(0.142 MeV)	(0.355 MeV)	(1.369 MeV)	(1.659 MeV)	(0.355 MeV)	(0.24 MeV)
0.10	4.89E-25	4.89E-25	2.67E-23	7.28E-19	7.46E-19	2.42E-18	3.85E-26
0.15	1.23E-20	9.47E-21	3.47E-17	3.37E-14	3.14E-14	2.35E-14	7.99E-18
0.20	2.60E-16	1.26E-16	9.63E-14	1.33E-11	1.31E-11	6.85E-12	1.02E-13
0.30	1.80E-11	5.22E-11	5.08E-10	1.47E-08	1.73E-08	7.02E-09	1.12E-09
0.40	4.25E-09	3.06E-08	4.67E-08	1.03E-06	1.44E-06	4.82E-07	1.63E-07
0.50	1.05E-07	1.31E-06	7.28E-07	1.99E-05	3.15E-05	8.94E-06	1.05E-05
0.60	8.55E-07	1.53E-05	4.51E-06	1.81E-04	3.16E-04	7.79E-05	2.51E-04
0.70	3.83E-06	8.54E-05	1.65E-05	1.02E-03	1.90E-03	4.19E-04	2.47E-03
0.80	1.26E-05	3.02E-04	4.35E-05	4.08E-03	7.97E-03	1.63E-03	1.35E-02
0.90	3.65E-05	7.92E-04	9.41E-05	1.28E-02	2.58E-02	4.97E-03	4.99E-02
1.00	1.01E-04	1.68E-03	1.82E-04	3.34E-02	6.86E-02	1.27E-02	1.40E-01
1.50	7.57E-03	1.47E-02	4.90E-03	7.81E-01	1.60E+00	2.90E-01	2.67E+00
2.00	1.29E-01	5.08E-02	8.28E-02	4.59E+00	8.79E+00	1.73E+00	1.03E+01
2.50	7.93E-01	1.79E-01	5.99E-01	1.48E+01	2.65E+01	5.55E+00	2.16E+01

The comparison between different rates relative to the present mirror rate is shown in Fig. 2. The differences are explained below: (1) the statistical-model rates (rath, ths8, thra) are about 1–6 orders of magnitude larger, which demonstrates that the statistical-model is not ideally applicable for this reaction mainly owing to the low density of low-lying excited states in ^{51}Co. (2) the laur rate based on the mirror information of ^{51}Cr is about a factor of 30–650 times larger at temperature >0.15 GK, mainly because of two factors: one is the different $S_{\rm p}$ values utilized, another is the inappropriate approximation ($\omega\gamma\approx\omega\Gamma_\gamma$) made in the previous work as discussed in Sec.2.2; below ~0.15 GK, laur rate decreases because its DC contribution was neglected [20]. (3) In the temperature region of 1–2.5 GK, the nfis rate is almost the closest one (with deviation less than ~50%) to the mirror rate; below 1 GK, nfis is about 1–3 orders magnitude smaller mainly because of a relatively larger

value of S_p=0.355 MeV utilized. (4) The present shell rate agrees with the mirror one within a factor of up to about 10.

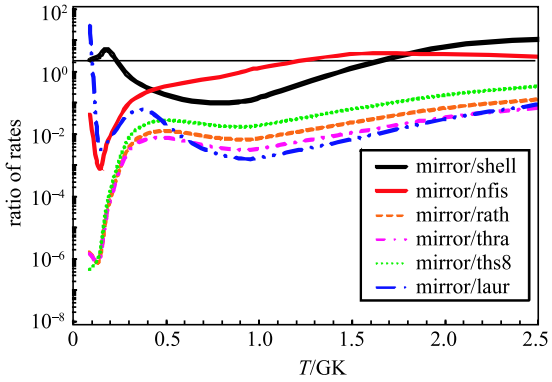

Fig. 2. (color online) Comparison between different reaction rates relative to the present mirror rate. The reference of unity is indicated by a solid line.

4 Summary

The thermonuclear rate (including direct-capture (DC) and resonant contribution) of the ^{50}Fe(p, γ)^{51}Co reaction has been recalculated by utilizing the recent precise proton separation energy of $S_p(^{51}\mathrm{Co})$=142±77 keV measured at the HIRFL-CSR facility in Lanzhou, China. Here, the resonant rates have been calculated in two ways: one is to revise the previous shell-model results with this new S_p value (i.e., shell rate), another is to rely on the mirror nuclear structure of ^{51}Cr (i.e., mirror rate). Our new rates deviate significantly from those available in the literature. We conclude that statistical model calculations are not ideally applicable for this reaction primarily because of the low density of low-lying excited states in ^{51}Co. Thus, we recommend that the present new mirror rate should be incorporated in future astrophysical network calculations, since it is based on a more solid experimental background. The astrophysical impact of our new rates in Type I X-ray burst calculations is now in progress, which is beyond the scope of this work.

References

1 S.E. Woosley and R.E. Taam, Nature, **263**: 101–103 (1976)
2 P.C. Joss, Nature, **270**: 310–314 (1977)
3 H. Schatz et al, Phys. Rev. Lett., **86**: 3471–3474 (2001)
4 V.-V. Elomaa et al, Phys. Rev. Lett., **102**: 252501 (2009)
5 R.K. Wallace and S.E. Woosley, Astrophys. J. Suppl., **45**: 389–420 (1981)
6 H. Schatz et al, Phys. Rep., **294**: 167–263 (1998)
7 S.E. Woosley et al, Astrophys. J. Suppl., **151**: 75–102 (2004)
8 W. Lewin et al, Space Sci. Rev., **62**: 223–389 (1993)
9 T. Strohmayer, L. Bildsten, in *Compact Stellar X-Ray Sources*, edited by W. Lewin and M. van der Klis (Cambridge: Cambridge Univ. Press, 2006)
10 A. Parikh et al, Prog. Part. Nucl. Phys., **69**: 225–253 (2013)
11 A. Parikh et al, Phys. Rev. C, **79**: 045802 (2009)
12 H. Schatz and K. E. Rehm, Nucl. Phys. A, **777**: 601–622 (2006)
13 J. W. Xia et al, Nucl. Instrum. Methods A, **488**: 11–25 (2002)
14 P. Shuai et al, Phys. Lett. B, **735**: 327–331 (2014)
15 A.H. Wapstra and G. Audi, Nucl. Phys. A, **432**: 1–54 (1985)
16 G. Audi and A.H. Wapstra, Nucl. Phys. A, **565**: 1–65 (1993)
17 G. Audi and A.H. Wapstra, Nucl. Phys. A, **595**: 409–480 (1995)
18 G. Audi, A.H. Wapstra, and C. Thibault, Nucl. Phys. A, **729**: 337–676 (2003)
19 J.J. He et al, Phys. Rev. C, **89**: 035802 (2014)
20 L. Van Wormer et al, Astrophy. J, **432**: 326–350 (1994)
21 T. Rauscher and F.-K. Thielemann, At. Data Nucl. Data Tables, **75**: 1–351 (2000)
22 T. Rauscher and F.-K. Thielemann, in *Stellar Evolution, Stellar Explosions and Galactic Chemical Evolution*, edited by A. Mezzacappa (IOP: Bristol, 1998)
23 P. Möller et al, At. Data Nucl. Data Tables, **59**: 185–381 (1995)
24 J.M. Pearson et al, Phys. Lett. B, **387**: 455–459 (1996)
25 J.L. Fisker et al, At. Data Nucl. Data Tables, **79**: 241–292 (2001)
26 R.H. Cyburt et al, Astrophys. J. Suppl., **189**: 240–252 (2010)
27 C.E. Rolfs and W.S. Rodney, *Cauldrons in the Cosmos* (Chicago: Univ. of Chicago Press, 1988)
28 J. José et al, Astrophys. J. Suppl., **189**: 204–239 (2010)
29 A.R. Barnett et al, Comput. Phys. Commun., **8**: 377–395 (1974)
30 X.L. Huang, Nucl. Data Sheets, **107**: 2131–2322 (2006)
31 J.E. Robertshaw et al, Phys. Rev., **170**: 1013–1033 (1968)
32 A.E. Macgregor and G. Brwon, Nucl. Phys. A, **190**: 548–564 (1972)
33 M.S. Chowdhury, A.R. Majumder, and H.M. Sen Gupta, Nucl. Phys. A, **282**: 87–108 (1977)
34 Z.D. Wu et al, Phys. Rev. C, **89**: 054315 (2014)
35 C.A. Bertulani, Comput. Phys. Commun., **156**: 123–141 (2003)
36 T. Rauscher, *EXP2RATE v2.1*, http://nucastro.org/codes.html
37 J.T. Huang, C.A. Bertulani, and V. Guimarães, At. Data Nucl. Data Tables, **96**: 824–847 (2010)